Optimal detection of metrologically useful entanglement

Iagoba Apellaniz,[1] Matthias Kleinmann,[1] Otfried Gühne,[2] and Géza Tóth[1, 3, 4]

[1] *Department of Theoretical Physics, University of the Basque Country UPV/EHU, E-48080 Bilbao, Spain*
[2] *Naturwissenschaftlich-Technische Fakultät, Universität Siegen, Walter-Flex-Str. 3, 57068 Siegen, Germany*
[3] *IKERBASQUE, Basque Foundation for Science, E-48013 Bilbao, Spain*
[4] *Wigner Research Centre for Physics, Hungarian Academy of Sciences, H-1525 Budapest, Hungary*

(Dated: May 11, 2019)

We show how to verify the metrological usefulness of quantum states based on few measurements. In particular, we estimate the quantum Fisher information as a figure of merit of metrological usefulness. Our approach is optimal since it gives a tight lower bound on the quantum Fisher information for the given incomplete information. We apply our method to the results of various multi-particle quantum states prepared in experiments with photons and trapped ions, as well as to spin-squeezed states and Dicke states realized in cold gases.

PACS numbers: 03.67.Mn, 03.75.Gg, 03.75.Dg, 42.50.St

arXiv:1511.05203v1 [quant-ph] 16 Nov 2015

Introduction.—Entanglement lies at the heart of many problems in quantum mechanics and has attracted increasing attention in recent years. There are now efficient methods to detect it with few measurements [1, 2]. However, in spite of intensive research, many of the intriguing properties of entanglement are not fully understood. One of such puzzling facts is that, while entanglement is a sought after resource, not all entangled states are useful for some particular quantum information processing task. For instance, it has been realized recently that entanglement is needed in very general metrological tasks to achieve a high precision [3]. Remarkably, this is true even in the case of millions of particles, which is especially important for characterizing the entanglement properties of cold atomic ensembles [4–9]. However, there are highly entangled pure states that are useless for metrology [10].

In the light of the these results, beside verifying that a quantum state is entangled, we should also show that it is useful for metrology. This is possible if we know the quantum Fisher information $\mathcal{F}_Q[\varrho, J_l]$ for the state. Here ϱ is a density matrix of an ensemble of N two-level systems (i.e., qubits), $J_l = \frac{1}{2}\sum_n \sigma_l^{(n)}$ for $l = x, y, z$ are the angular momentum components, and $\sigma_l^{(n)}$ are the Pauli spin matrices acting on qubit n. The quantity $\mathcal{F}_Q[\varrho, J_l]$ is a central notion of quantum metrology. It is connected to the task of estimating the phase θ for the unitary dynamics of a linear interferometer $U = \exp(-iJ_l\theta)$, starting from ϱ as the initial state. It provides a tight bound for the precision of phase estimation as [11, 12]

$$(\Delta\theta)^2 \geq \frac{1}{\mathcal{F}_Q[\varrho, J_l]}. \tag{1}$$

It has been shown that if $\mathcal{F}_Q[\varrho, J_l]$ is larger than the value achieved by product states [3] then the state ϱ is entangled. Higher values of the quantum Fisher information indicate even multipartite entanglement [13], this fact has been used to analyze several experiments [8, 9, 14].

Typically, we do not know the density matrix and we can only estimate the quantum Fisher information based on a couple of operator expectation values [15]. The archetypical criterion in this regard is [3]

$$\mathcal{F}_Q[\varrho, J_y] \geq \frac{\langle J_z\rangle^2}{(\Delta J_x)^2}, \tag{2}$$

which is expected to work best for states that are almost completely polarized in the z-direction and spin squeezed in the x-direction. Apart from spin-squeezed states, there are conditions similar to Eq. (2) for symmetric states close to Dicke states [16–19] and for two-mode squeezed states [20].

After finding criteria for various systems, it is crucial to develop a general method that provides an *optimal* lower bound on the quantum Fisher information in a wide class of cases, especially for the states most relevant for experiments such as spin-squeezed states [21], Greenberger-Horne-Zeilinger (GHZ) states [22], and symmetric Dicke states [16]. It seems that such a method would involve a numerical minimization over all density matrix elements constrained for some operator expectation values. Since finding the global minimum is not guaranteed, a trustable optimization would be impossible apart from very small systems.

In this paper, we demonstrate that tight lower bounds on the quantum Fisher information can still be computed efficiently. Remarkably, our method works for thousands of particles. We will show how to obtain a bound on the quantum Fisher information from fidelity measurements for GHZ states [23–30] and for symmetric Dicke states [14, 31–35]. We will also discuss how to obtain such bounds for spin-squeezed states of thousand of atoms [6, 7, 36] and for symmetric Dicke states prepared recently in cold gases [8, 37, 38].

Estimation of a general function of ϱ.—First, we review a state-of-the-art solution for the problem of finding a lower bound on a convex function $g(\varrho)$ based only on a single operator expectation value $w = \langle W\rangle_\varrho = \mathrm{Tr}(W\varrho)$. Theory tells us that a tight lower bound can be obtained

as [39–41]

$$g(\varrho) \geq \mathcal{B}(w) := \sup_r \left[rw - \hat{g}\left(rW\right)\right], \tag{3}$$

where $\hat{g}$ is the Legendre transform, in this context defined as

$$\hat{g}(W) = \sup_{\varrho}[\langle W\rangle_\varrho - g(\varrho)]. \tag{4}$$

Equation (3) has been applied to entanglement measures [40, 41]. Since those are defined as convex roofs over all possible decompositions of the density matrix, it is sufficient to carry out the optimization in Eq. (3) for pure states only. However, still an optimization over a general pure state, i.e., over many variables has to be carried out, which is practical only for small systems.

Estimation of the quantum Fisher information.— We would like to estimate the quantum Fisher information, which is strongly connected to entanglement, while it also has a clear physical meaning in metrological applications. As a first step, we note that $\mathcal{F}_Q[\varrho, J_l]$ can be obtained as a closed formula with ϱ and J_l [12], however, this is a highly nonlinear expression which would make the computation of the Legendre transform very demanding. A key point in our approach is using a very recent finding showing that $\mathcal{F}_Q[\varrho, J_l]$ is the convex roof of $4(\Delta J_y)^2$ [42], and hence the optimization may be carried out only for pure states. With this, however, we are still facing an optimization problem that cannot be solved numerically for system sizes relevant for quantum metrology.

We now arrive at our first main result. We show that Eq. (4) can be rewritten as an optimization over a *single* real parameter.

Observation 1.—The quantum Fisher information can be estimated using the Legendre transform

$$\hat{\mathcal{F}}_Q(W) = \sup_\mu \left\{\lambda_{\max}\left[W - 4(J_l - \mu)^2\right]\right\}, \tag{5}$$

where $\lambda_{\max}(A)$ denotes the maximal eigenvalue of A.

Proof. Based on the previous discussion, we can rewrite the right-hand side of Eq. (4) for our case as

$$\hat{\mathcal{F}}_Q(W) = \sup_\Psi[\langle W - 4J_l^2\rangle_\Psi + 4\left\langle J_l\right\rangle_\Psi^2]. \tag{6}$$

Equation (6) is quadratic in operator expectation values. It can be rewritten as an optimization linear in operator expectation values as

$$\hat{\mathcal{F}}_Q(W) = \sup_{\Psi,\mu}[\langle W - 4J_l^2\rangle_\Psi + 8\mu\left\langle J_l\right\rangle_\Psi - 4\mu^2], \tag{7}$$

which can be reformulated as Eq. (5). At the extremum, the derivative with respect to μ must be zero, hence at the optimum $\mu = \left\langle J_l\right\rangle_\Psi$. This also means that we have to test μ values in the interval $-N/2 \leq \mu \leq N/2$ only. ■

The full optimization problem to be solved consists of Eq. (5), and Eq. (3) with the substitutions $g(\varrho) = F_Q[\varrho, J_l]$ and $\hat{g}(W) = \hat{\mathcal{F}}_Q(W)$. It is crucial that the optimization in Eq. (3) is over a concave function, since $\hat{\mathcal{F}}_Q(rW)$ is a convex function in r [39]. Thus the optimum can be determined easily with simple methods, e.g., the gradient method, looking for the maximum in r. Based on Eq. (3), we can see that even if we do not find the global optimum in r, we obtain a valid lower bound.

We want to stress the generality of our findings beyond linear interferometers covered in this article. For nonlinear interferometers [43–48], the phase θ must be estimated in a unitary dynamics $U = \exp(-iA\theta)$, where A is not a sum of single spin operators, hence, is different from the angular momentum components. Using Observation 1, we can obtain lower bounds for the corresponding quantum Fisher information $\mathcal{F}_Q[\varrho, A]$, if we replace J_l by A in Eq. (5).

Next, we will demonstrate the use of our approach for several experimentally relevant situations. In the many-particle case, often symmetric operators can be used, which makes it possible to carry out calculations for thousands of particles.

Fidelity measurements.—Let us consider the case when W is a projector onto a pure quantum state. First, we consider GHZ states [22]. We choose $W = |\mathrm{GHZ}\rangle\langle\mathrm{GHZ}|$, hence $\langle W\rangle$ is equal to F_{GHZ}, the fidelity with respect to the GHZ state. Based on knowing F_{GHZ}, we would like to estimate $\mathcal{F}_Q[\varrho, J_z]$.

Observation 2.—A sharp lower bound on the quantum Fisher information with the fidelity F_{GHZ} is given by

$$\frac{\mathcal{F}_Q[\varrho, J_z]}{N^2} \geq \begin{cases} (1 - 2F_{\mathrm{GHZ}})^2, & \text{if } F_{\mathrm{GHZ}} > 1/2, \\ 0, & \text{if } F_{\mathrm{GHZ}} \leq 1/2. \end{cases} \tag{8}$$

The proof is based on carrying out the optimization described above analytically, and can be found in the Supplement [49]. Equation (8) is plotted in Fig. 1(a). Note that the bound on the quantum Fisher information normalized by N^2 in Eq. (8) is independent of the number of particles. Moreover, the bound is zero for $F_{\mathrm{GHZ}} \leq 0.5$. This is consistent with the fact that for the product state $|111...11\rangle$ we have $F_{\mathrm{GHZ}} = 0.5$, while $\mathcal{F}_Q[\varrho, J_z] = 0$.

Next, let us consider symmetric Dicke states. An N-qubit symmetric Dicke state is given as

$$|\mathrm{D}_N^{(m)}\rangle = \binom{N}{m}^{-\frac{1}{2}} \sum_k \mathcal{P}_k(|1\rangle^{\otimes m} \otimes |0\rangle^{\otimes(N-m)}), \tag{9}$$

where the summation is over all the different permutations of the product state having m particles in the $|1\rangle$ state and $(N - m)$ particles in the $|0\rangle$ state.

From the point of view of metrology, we are interested mostly in the symmetric Dicke state for even N and $m = \frac{N}{2}$. This state is known to be highly entangled [53, 54] and allows for Heisenberg limited interferometry [55]. In the following, we will omit the superscript giving the number

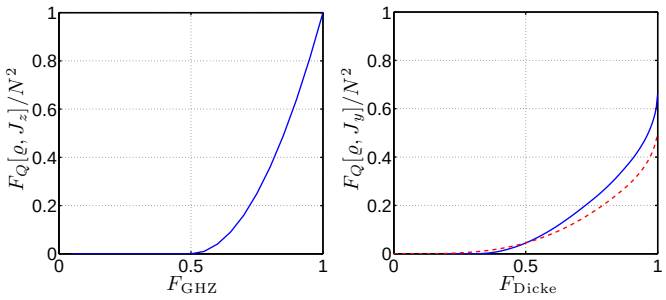

FIG. 1. (Color online) Fidelity vs. lower bound on the quantum Fisher information (a) for GHZ states of N qubits. The quantum Fisher information is zero if the fidelity is smaller than 0.5. (b) The same for Dicke states for (solid) $N = 6$ and (dashed) $N = 40$.

of $|1\rangle$'s and use the notation

$$|\mathrm{D}_N\rangle \equiv |\mathrm{D}_N^{(\frac{N}{2})}\rangle. \tag{10}$$

In Fig. 1(b), we plotted the results for symmetric Dicke states of various number of qubits. Now the normalized curve is not the same for all particle numbers. $F_{\rm Dicke} = 1$ corresponds to $F_Q[\varrho, J_y] = N(N+2)/2$ [13]. At this point note that for the examples presented above, the quantum Fisher information scales as $O(N^2)$ if the quantum state has been prepared perfectly, where $O(x)$ is the usual Landau notation used to describe the asymptotic behavior of a quantity for large x [13].

When making calculations for quantum systems with an increasing number of qubits, we soon run into difficulties when computing the largest eigenvalue of Eq. (5). The reason is that for N qubits, we need to handle $2^N \times 2^N$ matrices, hence we are limited to systems of $10 - 15$ qubits. We can obtain bounds for much larger particle numbers, if we restrict ourselves to the symmetric subspace [50]. This approach can give optimal bounds for many systems, such as Bose-Einstein condensates of two-state atoms, which are in a symmetric multiparticle state. The bound computed for the symmetric subspace might be not correct for general states. However, if the operator W is permutationally invariant and the eigenstate with the maximal eigenvalue of the matrix in Eq. (5) is non-degenerate, then the two coincide [49]. This is the case when estimating $\mathcal{F}_Q[\varrho, J_y]$ based on $F_{\rm Dicke}$, hence it was possible to carry out calculations for 40 qubits for Fig. 1(b) and the bound is valid even for general, i.e., non-symmetric states. Calculations for the large $N-$limit can be found in the Supplement [49].

Multiparticle entanglement vs. quantum Fisher information.—The bounds on the quantum Fisher information make it possible to detect metrologically useful entanglement. It has been shown that if $\mathcal{F}_Q[\varrho, J_l] > (k-1)N$, where k is an integer, then the state possesses at least k-particle entanglement [3, 13]. We can immediately see, that perfect GHZ and $|\mathrm{D}_N\rangle$ states possess metrologically useful N-particle entanglement. Based on the ideas above, it is possible to use the quantum Fisher information for entanglement detection [8, 9, 14]. Typically the conditions for metrologically useful k-particle entanglement are much stricter than for k-particle entanglement. The reason is that in order to obtain metrologically useful k-particle entanglement, the state must outperform a tensor product of GHZ-states of $(k-1)$-particles [56].

Measuring several observables.—So far, we studied the quantum state of few particles. Next we will turn to experiments with very many particles, in which a fidelity measurement is not practical. In such systems, the quantum Fisher information must be estimated based on several collective measurements. Thus, we have to formulate our approach for the multivariable case.

We can generalize Eqs. (3) and (4) for measuring several observables W_k as [40]

$$\mathcal{F}_Q[\varrho, J_y] \geq \sup_{r_1, r_2, \ldots, r_K} \left[\sum_{k=1}^{K} r_k w_k - \hat{\mathcal{F}}_Q \left(\sum_{k=1}^{K} r_k W_k \right) \right], \tag{11}$$

where $w_k = \langle W_k \rangle_\varrho$. In this case, we will have several parameters r_k. Nevertheless, the optimum can easily be obtained with the gradient method, since the right-hand side of Eq. (11) is concave in r_k, since $\hat{\mathcal{F}}_Q\left(\sum_k r_k W_k\right)$ is convex in r_k [39]. For clarity, we also give a single formula for the entire optimization problem that has to be solved for obtaining the bound in the multivariable case in the Supplement [49].

By far the most relevant quantum state in many-particle experiments are spin-squeezed states that can be used to increase the precision in magnetometry and in atomic clocks [57].

Spin-squeezed states.—In the case of spin squeezing, the quantum state has a large spin in the z-direction, while a decreased variance in the x-direction. By measuring $\langle J_z \rangle$ and $(\Delta J_x)^2$ we can estimate the quantum Fisher information by Eq. (2). However, this formula does not necessarily give the best lower bound for all values of the collective observables. With our approach we can find the best bound.

To give a concrete example, we choose $W_1 = J_z$, $W_2 = J_x^2$ and $W_3 = J_x$ for the operators to be measured. We change w_1 and w_2 in some interval. We also require that $w_3 = 0$, since we assume that the mean spin points into the z-direction [58]. This is reasonable since in most spin-squeezing experiments we know the direction of the mean spin. Our results can be seen in Fig. 2(a). We chose $N = 4$ particles since for small N the main features of the plot are clearly visible. The white areas correspond to non-physical combination of expectation values. States at the boundary can be obtained as ground states of $H_{\rm bnd}^{(\pm)}(\mu) = \pm J_x^2 - \mu J_z$ [49]. In Fig. 2(a), the state fully polarized in the z-direction, an

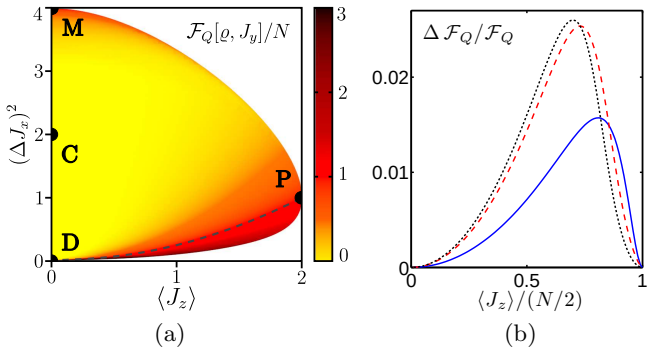

(a) (b)

FIG. 2. (Color online) (a) Optimal lower bound on the quantum Fisher information $\mathcal{F}_Q[\varrho, J_y]$ based on collective measurements for spin-squeezing for $N = 4$. We assume that the mean spin points into the z-direction. Below the dashed line $\mathcal{F}_Q[\varrho, J_y]/N > 1$. For the description of points P, D, M, and C, see text. (b) Relative difference $\Delta\mathcal{F}_Q/\mathcal{F}_Q$ between our bound for states at the boundary of physical states and the bound in Eq. (2) for boundary points below point P for (solid) $N = 4$, (dashed) $N = 20$, and (dotted) $N = 1000$.

initial state for spin-squeezing experiments, corresponds to point P. The Dicke state (10) corresponds to point D [59]. Spin squeezing makes $(\Delta J_x)^2$ decrease, while $\langle J_z \rangle$ also decreases somewhat. Hence, at least for small squeezing, it corresponds to moving down from point P towards point D on the boundary of the plot, while the metrological usefulness is increasing. Below the dashed line $\mathcal{F}_Q[\varrho, J_y]/N > 1$, hence the state possesses metrologically useful entanglement [3]. The equal mixture of $|000..00\rangle_x$ and $|111..11\rangle_x$ corresponds to point M, with $F_Q[\varrho_M, J_y] = N$. Finally, the completely mixed state corresponds to point C. It cannot be used for metrology, hence $\mathcal{F}_Q[\varrho_C, J_y] = 0$.

We now compare the difference between our bound and Eq. (2). First, we consider the experimentally relevant region for which $(\Delta J_x)^2 < 1$. We find that for points that are away from the boundary at least by 0.01 on the vertical axis, the difference between the two bounds for $F_Q[\varrho, J_y]$ is smaller than 2×10^{-6}. For points at the boundary the difference is somewhat larger, but still small. The relative difference is less than 2%, and remains small even for larger particle numbers as shown in Fig. 2(b). Hence, Eq. (2) practically coincides with the optimal bound for $(\Delta J_x)^2 < 1$. We now consider the region in Fig. 2(a) for which $(\Delta J_x)^2 > 1$. The difference between the two bounds is now larger. It is largest at point M, for which the bound (2) is zero. Hence, for measurement values corresponding to points close to M, our method could improve the formula (2).

Calculations for experimental data.— Our results concerning the analysis of experimental data, giving the details in the Supplement [49], are the following. (i) We determined the quantum Fisher information for several experiments in photons and trapped ions creating GHZ states and Dicke states, in which the fidelity has been measured [14, 25, 27–34, 60–63], which is much easier than obtaining the quantum Fisher information from the density matrix [14], or estimating it from a metrological procedure [8]. (ii) We could obtain a bound on the quantum Fisher information for a spin-squeezing experiment with thousands of particles [7]. Based on numerical examples, we see that the bound (2) is close to optimal for large N, even for not completely polarized states. (iii) We obtained the bound for the quantum Fisher information for a recent experiment with Dicke states [37]. The estimate of the precision based on considering the particular case when $\langle J_z^2 \rangle$ is measured for parameter estimation [19] is close to the optimal bound computed by our method.

Scaling of $\mathcal{F}_Q[\varrho, J_l]$ with N.—Recent important works examine the scaling of the quantum Fisher information with the particle number for metrology under the presence of decoherence [64]. They consider the quantum Fisher information defined now for the non-unitary, noisy evolution. They find that for small N it is close to the value obtained by considering coherent dynamics. Hence, even the Heisenberg scaling, $O(N^2)$, can be reached. However, if N is sufficiently large then, due to the decoherence during the parameter estimation, the quantum Fisher information scales as $O(N)$.

We have to stress that the findings of Ref. [64] are not applicable for our case. Our method estimates the quantum Fisher information assuming a perfect unitary dynamics. The quantum Fisher information can be smaller than what we expect ideally only due to the imperfect state preparation [65]. We can even find simple conditions on the state preparation that lead to a Heisenberg scaling. Based on Eq. (8), if one could realize quantum states ϱ_N such that $F_{\rm GHZ}(\varrho_N) \geq 0.5 + \epsilon$ for $N \to \infty$ for some $\epsilon > 0$, then we would reach $\mathcal{F}_Q[\varrho_N, J_z] = O(N^2)$. Strong numerical evidence suggests that a similar relation holds for the fidelity $F_{\rm Dicke}$ and $\mathcal{F}_Q[\varrho_N, J_y]$, but with a smaller threshold value for $F_{\rm Dicke}$ [49].

Conclusions.—We showed a general method to estimate the metrological usefulness of quantum states based on few measurements, such as measuring the fidelity or some collective observables. We tested our approach on extensive experimental data on photonic and cold gas experiments, and demonstrated that it works even for the case of thousands particles [66]. In the future, it would be interesting to use our method to test the optimality of various recent formulas giving a lower bound on the quantum Fisher information [17, 20], as well as to improve the lower bounds for spin-squeezed states and Dicke states allowing for the measurement of more observables than the ones used in this publication.

We thank S. Altenburg, F. Fröwis, R. Demkowicz-Dobrzański, P. Hyllus, J. Kołodiński, M.W. Mitchell, M. Modugno, L. Pezze, L. Santos, A. Smerzi, I. Urizar-Lanz, and G. Vitagliano for stimulating discussions. We thank the organizers and the participants of the

589. Heraeus-Seminar on "Continuous Variable Entanglement in Atomic Systems" for scientific exchange. We acknowledge the support of the EU (ERC Starting Grant 258647/GEDENTQOPT, CHIST-ERA QUASAR, Marie Curie CIG 293993/ENFOQI), the MINECO (Project No. FIS2012-36673-C03-03), the Basque Government (Project No. IT4720-10), the OTKA (Contract No. K83858), the UPV/EHU program UFI 11/55, the FQXi Fund (Silicon Valley Community Foundation), and the DFG (Forschungsstipendium KL 2726/2-1).

[1] R. Horodecki, P. Horodecki, M. Horodecki, and K. Horodecki, Rev. Mod. Phys. **81**, 865 (2009).
[2] O. Gühne and G. Tóth, Phys. Rep. **474**, 1 (2009).
[3] L. Pezzé and A. Smerzi, Phys. Rev. Lett. **102**, 100401 (2009).
[4] A. Louchet-Chauvet, J. Appel, J. J. Renema, D. Oblak, N. Kjaergaard, and E. S. Polzik, New J. Phys. **12**, 065032 (2010).
[5] J. Appel, P. J. Windpassinger, D. Oblak, U. B. Hoff, N. Kjærgaard, and E. S. Polzik, PNAS **106**, 10960 (2009).
[6] M. F. Riedel, P. Böhi, Y. Li, T. W. Hänsch, A. Sinatra, and P. Treutlein, Nature **464**, 1170 (2010).
[7] C. Gross, T. Zibold, E. Nicklas, J. Esteve, and M. K. Oberthaler, Nature **464**, 1165 (2010).
[8] B. Lücke, M. Scherer, J. Kruse, L. Pezzé, F. Deuretzbacher, P. Hyllus, J. Peise, W. Ertmer, J. Arlt, L. Santos, A. Smerzi, and C. Klempt, Science **334**, 773 (2011).
[9] H. Strobel, W. Muessel, D. Linnemann, T. Zibold, D. B. Hume, L. Pezzé, A. Smerzi, and M. K. Oberthaler, Science **345**, 424 (2014).
[10] P. Hyllus, O. Gühne, and A. Smerzi, Phys. Rev. A **82**, 012337 (2010).
[11] V. Giovannetti, S. Lloyd, and L. Maccone, Science **306**, 1330 (2004); M. G. A. Paris, Int. J. Quant. Inf. **07**, 125 (2009); R. Demkowicz-Dobrzanski, M. Jarzyna, and J. Kolodynski, Prog. Optics, **60**, 345 (2015), arXiv:1405.7703; L. Pezze and A. Smerzi, in *Atom Interferometry (Proc. Int. School of Physics 'Enrico Fermi', Course 188, Varenna)* edited by G. Tino and M. Kasevich (IOS Press, Amsterdam, 2014) pp. 691–741, arXiv:1411.5164.
[12] C. Helstrom, *Quantum Detection and Estimation Theory* (Academic Press, New York, 1976); A. Holevo, *Probabilistic and Statistical Aspects of Quantum Theory* (North-Holland, Amsterdam, 1982); S. L. Braunstein and C. M. Caves, Phys. Rev. Lett. **72**, 3439 (1994); D. Petz, *Quantum information theory and quantum statistics* (Springer, Berlin, Heilderberg, 2008); S. L. Braunstein, C. M. Caves, and G. J. Milburn, Ann. Phys. **247**, 135 (1996).
[13] P. Hyllus, W. Laskowski, R. Krischek, C. Schwemmer, W. Wieczorek, H. Weinfurter, L. Pezzé, and A. Smerzi, Phys. Rev. A **85**, 022321 (2012); G. Tóth, Phys. Rev. A **85**, 022322 (2012).
[14] R. Krischek, C. Schwemmer, W. Wieczorek, H. Weinfurter, P. Hyllus, L. Pezzé, and A. Smerzi, Phys. Rev. Lett. **107**, 080504 (2011).
[15] In another context, the measurement of the quantum Fisher information has recently been considered in systems in thermal equilibrium. P. Hauke, M. Heyl, L. Tagliacozzo, and P. Zoller, arXiv:1509.01739.
[16] R. H. Dicke, Phys. Rev. **93**, 99 (1954).
[17] Z. Zhang and L. M. Duan, New J. Phys. **16**, 103037 (2014).
[18] F. Fröwis and N. Gisin, arXiv:1409.4440.
[19] I. Apellaniz, B. Lücke, J. Peise, C. Klempt, and G. Tóth, New J. Phys. **17**, 083027 (2015).
[20] E. Oudot, P. Sekatski, F. Fröwis, N. Gisin, and N. Sangouard, arXiv:1410.8421.
[21] M. Kitagawa and M. Ueda, Phys. Rev. A **47**, 5138 (1993); D. J. Wineland, J. J. Bollinger, W. M. Itano, and D. J. Heinzen, Phys. Rev. A **50**, 67 (1994).
[22] D. M. Greenberger, M. A. Horne, A. Shimony, and A. Zeilinger, Am. J. Phys. **58**, 1131 (1990).
[23] D. Bouwmeester, J.-W. Pan, M. Daniell, H. Weinfurter, and A. Zeilinger, Phys. Rev. Lett. **82**, 1345 (1999).
[24] J.-W. Pan, D. Bouwmeester, M. Daniell, H. Weinfurter, and A. Zeilinger, Nature **403**, 515 (2000).
[25] Z. Zhao, T. Yang, Y.-A. Chen, A.-N. Zhang, M. Żukowski, and J.-W. Pan, Phys. Rev. Lett. **91**, 180401 (2003).
[26] C.-Y. Lu, X.-Q. Zhou, O. Gühne, W.-B. Gao, J. Zhang, Z.-S. Yuan, A. Goebel, T. Yang, and J.-W. Pan, Nat. Phys. **3**, 91 (2007).
[27] W.-B. Gao, C.-Y. Lu, X.-C. Yao, P. Xu, O. Gühne, A. Goebel, Y.-A. Chen, C.-Z. Peng, Z.-B. Chen, and J.-W. Pan, Nat. Phys. **6**, 331 (2010).
[28] D. Leibfried, M. Barrett, T. Schaetz, J. Britton, J. Chiaverini, W. Itano, J. Jost, C. Langer, and D. Wineland, Science **304**, 1476 (2004).
[29] C. Sackett, D. Kielpinski, B. King, C. Langer, V. Meyer, C. Myatt, M. Rowe, Q. Turchette, W. Itano, D. Wineland, and C. Monroe, Nature **404**, 256 (2000).
[30] T. Monz, P. Schindler, J. T. Barreiro, M. Chwalla, D. Nigg, W. A. Coish, M. Harlander, W. Hänsel, M. Hennrich, and R. Blatt, Phys. Rev. Lett. **106**, 130506 (2011).
[31] N. Kiesel, C. Schmid, G. Tóth, E. Solano, and H. Weinfurter, Phys. Rev. Lett. **98**, 063604 (2007).
[32] W. Wieczorek, R. Krischek, N. Kiesel, P. Michelberger, G. Tóth, and H. Weinfurter, Phys. Rev. Lett. **103**, 020504 (2009).
[33] R. Prevedel, G. Cronenberg, M. S. Tame, M. Paternostro, P. Walther, M. S. Kim, and A. Zeilinger, Phys. Rev. Lett. **103**, 020503 (2009).
[34] A. Chiuri, C. Greganti, M. Paternostro, G. Vallone, and P. Mataloni, Phys. Rev. Lett. **109**, 173604 (2012).
[35] P. Schindler, M. Müller, D. Nigg, J. T. Barreiro, E. Martinez, M. Hennrich, T. Monz, S. Diehl, P. Zoller, and R. Blatt, Nat. Phys. **9**, 361 (2013).
[36] C. Gross, J. Phys. B: At. Mol. Opt. Phys. **45**, 103001 (2012); J. Ma, X. Wang, C. P. Sun, and F. Nori, Phys. Rep. **509**, 89 (2011); J. Hald, J. L. Sørensen, C. Schori, and E. S. Polzik, Phys. Rev. Lett. **83**, 1319 (1999); R. J. Sewell, M. Koschorreck, M. Napolitano, B. Dubost, N. Behbood, and M. W. Mitchell, Phys. Rev. Lett. **109**, 253605 (2012).
[37] B. Lücke, J. Peise, G. Vitagliano, J. Arlt,

L. Santos, G. Tóth, and C. Klempt, Phys. Rev. Lett. **112**, 155304 (2014).
[38] C. Hamley, C. Gerving, T. Hoang, E. Bookjans, and M. Chapman, Nat. Phys. **8**, 305 (2012).
[39] R. T. Rockafellar, *Convex analysis* (Princeton University Press, Princeton, 2015).
[40] O. Gühne, M. Reimpell, and R. F. Werner, Phys. Rev. Lett. **98**, 110502 (2007).
[41] J. Eisert, F. G. S. L. Brandao, and K. M. R. Audenaert, New J. Phys. **9**, 46 (2007).
[42] G. Tóth and D. Petz, Phys. Rev. A **87**, 032324 (2013); S. Yu, arXiv:1302.5311.
[43] A. Luis, Physics Letters A **329**, 8 (2004).
[44] S. Boixo, S. T. Flammia, C. M. Caves, and J. Geremia, Phys. Rev. Lett. **98**, 090401 (2007).
[45] S. Choi and B. Sundaram, Phys. Rev. A **77**, 053613 (2008).
[46] S. M. Roy and S. L. Braunstein, Phys. Rev. Lett. **100**, 220501 (2008).
[47] M. Napolitano, M. Koschorreck, B. Dubost, N. Behbood, R. Sewell, and M. W. Mitchell, Nature **471**, 486 (2011).
[48] M. J. W. Hall and H. M. Wiseman, Phys. Rev. X **2**, 041006 (2012).
[49] For details, see the Supplemental Material at http://www.www.www, including Refs. [50–52].
[50] A. S. Sørensen and K. Mølmer, Phys. Rev. Lett. **86**, 4431 (2001).
[51] J. I. Cirac, A. K. Ekert, and C. Macchiavello, Phys. Rev. Lett. **82**, 4344 (1999).
[52] For MATLAB R2015a, see `http://www.mathworks.com`.
[53] G. Tóth, J. Opt. Soc. Am. B **24**, 275 (2007).
[54] G. Tóth, W. Wieczorek, R. Krischek, N. Kiesel, P. Michelberger, and H. Weinfurter, New J. Phys. **11**, 083002 (2009).
[55] M. J. Holland and K. Burnett, Phys. Rev. Lett. **71**, 1355 (1993).
[56] J.K. Thompson, private communication (2014).
[57] A. Sørensen, L.-M. Duan, J. Cirac, and P. Zoller, Nature **409**, 63 (2001).
[58] Due to symmetries of the problem, when minimzing $F_Q[\varrho, J_y]$ with the constrains on $\langle J_z\rangle$ and $\langle J_x^2\rangle$, we do not have to add explicitly the constraint $\langle J_x\rangle = 0$. Optimization with only the first two constraints will give the same bound [49].
[59] Outside the symmetric subspace, there are other states with $\langle J_l\rangle = 0$. For example, such a state is the multiparticle singlet. However, usual spin-squeezing procedures remain in the symmetric subspace, thus we discuss only the Dicke state.
[60] G. Tóth, W. Wieczorek, D. Gross, R. Krischek, C. Schwemmer, and H. Weinfurter, Phys. Rev. Lett. **105**, 250403 (2010).
[61] Z. Zhao, Y.-A. Chen, A.-N. Zhang, T. Yang, H. J. Briegel, and J.-W. Pan, Nature **430**, 54 (2004).
[62] Y.-F. Huang, B.-H. Liu, L. Peng, Y.-H. Li, L. Li, C.-F. Li, and G.-C. Guo, Nat. Commun. **2**, 546 (2011).
[63] D. Leibfried, E. Knill, S. Seidelin, J. Britton, R. B. Blakestad, J. Chiaverini, D. B. Hume, W. M. Itano, J. D. Jost, C. Langer, R. Ozeri, R. Reichle, and D. J. Wineland, Nature **438**, 639 (2005).
[64] B. Escher, R. de Matos Filho, and L. Davidovich, Nat. Phys. **7**, 406 (2011); R. Demkowicz-Dobrzański, J. Kołodyński, and M. Guţă, Nat. Commun. **3**, 1063 (2012).
[65] This is also a relevant observation for R. Augusiak, J. Kolodynski, A. Streltsov, M. Nath Bera, A. Acin, and M. Lewenstein, arXiv:1506.08837, where $\mathcal{F}_Q = O(N^2)$ is reached with weakly entangled states.
[66] For some of the programs used for this article, see the actual version of the QUBIT4MATLAB package at `http://www.mathworks.com/matlabcentral/`. The 3.0 version of the package is described in G. Tóth, Comput. Phys. Commun. **179**, 430 (2008) .

SUPPLEMENTAL MATERIAL

In this supplemental material, we give some further details of our derivations, and summarize some relevant experimental results.

S1. EXPLICIT FORM OF THE EXPRESSION TO BE OPTIMIZED

Here, in order to help the application of our method, we write down explicitly, what has to be optimized to find a lower bound on the quantum Fisher information.

Let us consider the single-variable case. The bound is given in Eq. (3), where the Legendre transform is defined in Eq. (5). Combining the two, we obtain that the estimation based on a single expectation value is

$$\mathcal{F}_Q[\varrho, J_l] \geq \sup_r \left[rw - \sup_\mu \lambda_{\max} \left(rW - 4J_l^2 + 8\mu J_l - 4\mu^2 \right) \right]. \tag{S1}$$

Next, let us see the estimation of the quantum Fisher information based on several expectation values. The bound for the multivariable case is given in Eq. (11). Combining it with the Legendre transform (5), we arrive at the formula

$$\mathcal{F}_Q[\varrho, J_l] \geq \sup_{\{r_k\}} \left[\sum_k r_k w_k - \sup_\mu \lambda_{\max}(M) \right], \tag{S2}$$

where

$$M = \sum_k r_k W_k - 4J_l^2 + 8\mu J_l - 4\mu^2. \tag{S3}$$

Based on the theory of Legendre transforms, the quantity to be maximized in r_k is convex [39], thus we can easily find the maximum. If we do not find the optimal r_k then we underestimate the real bound. Hence, we will still have a valid lower bound.

This does not hold for the optimization over μ. The function to be optimized is not a convex function of μ, and not finding the optimal μ leads to overestimating the bound. Thus, a large care must be taken especially when optimizing over μ.

S2. PROOF OF OBSERVATION 2

In this section, using Eqs. (3) and (5), we will obtain analytically a tight lower bound on the quantum Fisher information based on the fidelity with respect to the GHZ state, $F_{\rm GHZ}$.

The calculation that we have to carry out is computing the bound

$$\mathcal{B}(F_{\rm GHZ}) = \sup_r \{ rF_{\rm GHZ} - \sup_\mu [\lambda_{\max}(M_{\rm GHZ})] \}, \tag{S4}$$

where

$$M_{\rm GHZ} = r|{\rm GHZ}\rangle\langle{\rm GHZ}| - 4(J_z - \mu)^2 \mathbb{1}. \tag{S5}$$

We will make our calculations in the J_z basis, which is defined with the 2^N basis vectors $b_0 = |00...000\rangle$, $b_1 = |00...001\rangle$, $b_2 = |00...010\rangle$,..., $b_{(2^N-2)} = |11...110\rangle$, and $b_{(2^N-1)} = |11...111\rangle$. It is easy to see that the matrix (S5) is almost diagonal in the J_z basis. To be more specific, it can then be written as

$$M_{\rm GHZ} = M_{2\times 2} \oplus D, \tag{S6}$$

where $\oplus$ denotes the direct sum and

$$M_{2\times 2} = \begin{pmatrix} \frac{r}{2} - 4(\frac{N}{2} - \mu)^2 & \frac{r}{2} \\ \frac{r}{2} & \frac{r}{2} - 4(\frac{N}{2} + \mu)^2 \end{pmatrix} \tag{S7}$$

is given in the $\{b_0, b_{(2^N-1)}\}$ basis, while D is a diagonal matrix given in the basis of the rest of the b_k vectors as

$$D_k = -4(\langle b_k|J_z|b_k\rangle - \mu)^2 \tag{S8}$$

for $k = 1, 2, ..., (2^N - 2)$. This means that $M_{\rm GHZ}$ can be diagonalized as

$$\mathrm{diag}[\lambda_+, \lambda_-, D_1, D_2, ..., D_{(2^N-2)}], \tag{S9}$$

where the two eigenvalues of $M_{2\times 2}$ are

$$\lambda_\pm = \frac{r}{2} - N^2 - 4\mu^2 \pm \sqrt{16\mu^2 N^2 + \frac{r^2}{4}}. \tag{S10}$$

Next, we show a way that can simplify our calculations considerably. As indicated in Eq. (S4), we have to look for the maximal eigenvalue of $M_{\rm GHZ}$ and then optimize it over μ. We exchange the order of the two steps, that is, we look for the maximum of each eigenvalue over μ, and then find the maximal one. Clearly, based on Eq. (S8) we obtain

$$\sup_\mu D_k = 0, \tag{S11}$$

since we can always choose a value for μ that makes D_k zero, while it is clear, that it cannot be positive. Due this, the maximal eigenvalue, maximized also over μ, can be obtained as

$$\begin{aligned} \sup_\mu [\lambda_{\max}(M_{\rm GHZ})] &:= \max[0, \sup_\mu(\lambda_+)] \\ &= \begin{cases} 0, & \text{if } r < 0, \\ \frac{r}{2} + \frac{r^2}{16N^2}, & \text{if } 0 \leq r \leq 4N^2, \\ -N^2 + r, & \text{if } r > 4N^2, \end{cases} \end{aligned} \tag{S12}$$

where we did not have to look for the maximum of λ_- over μ since clearly $\lambda_+ \geq \lambda_-$. Finally, we have to substitute Eq. (S12) into Eq. (S4), and carry out the optimization over r, considering $F_{\rm GHZ} \in [0, 1]$. This way we arrive at Eq. (8).

S3. CALCULATIONS IN THE SYMMETRIC SUBSPACE

In this section we prove that if a permutationally invariant N-qubit Hamiltonian H has a nondegenerate ground state, then the ground state is in the symmetric subspace if $N > 2$. An analogous statement holds for the maximal eigenvalue. This is a well-known fact, we give a proof only for completeness.

Let us denote the non-degenerate ground state by $|\Psi\rangle$. This is at the same time the $T = 0$ thermal ground state, hence it must be a permutationally invariant pure state. For such states $S_{kl}|\Psi\rangle\langle\Psi|S_{kl} = |\Psi\rangle\langle\Psi|$, where S_{kl} is the swap operator exchanging qubits k and l. Based on this, follows that $S_{kl}|\Psi\rangle = c_{kl}|\Psi\rangle$, and $c_{kl} \in \{-1, +1\}$. There are three possible cases to consider.

(i) All $c_{kl} = +1$. In this case, for all permutation operators Π_j we have

$$\Pi_j|\Psi\rangle = |\Psi\rangle, \tag{S13}$$

since any permutation operator Π_j can be constructed as $\Pi_j = S_{k_1l_1}S_{k_2l_2}S_{k_3l_3\ldots}S_{k_ml_m}$, where $m \geq 1$. Equation (S13) means that the state $|\Psi\rangle$ is symmetric.

(ii) All $c_{kl} = -1$. This means that the state is antisymmetric, however, such a state exists only for $N = 2$ qubits.

(iii) Not all c_{kl} are the identical to each other. In this case, there must be k_+, l_+, k_-, l_- such that

$$\begin{aligned} S_{k_+l_+}|\Psi\rangle &= +|\Psi\rangle, \\ S_{k_-l_-}|\Psi\rangle &= -|\Psi\rangle. \end{aligned} \tag{S14}$$

Let us assume that k_+, l_+, k_-, l_- are indices different from each other. In this case, $|\Psi'\rangle = S_{k_+k_-}S_{l_+l_-}|\Psi\rangle$ is another ground state of the Hamiltonian H such that

$$\begin{aligned} S_{k_+l_+}|\Psi'\rangle &= -|\Psi'\rangle, \\ S_{k_-l_-}|\Psi'\rangle &= +|\Psi'\rangle. \end{aligned} \tag{S15}$$

Comparing Eq. (S14) and Eq. (S15) we can conclude that $|\Psi'\rangle \neq |\Psi\rangle$, while due to the permutational invariance of H we have $\langle\Psi|H|\Psi\rangle = \langle\Psi'|H|\Psi'\rangle$. Thus, $|\Psi\rangle$ is not a nongenerate ground state. Let us now see what happens if k_+, l_+, k_-, l_- are not all different from each other. The proof works in an analogous way for the only nontrivial case $k_+ = k_-$, when $S_{k_+k_-} = \mathbb{1}$.

Hence, if $N > 2$ then only (i) is possible and $|\Psi\rangle$ must be symmetric. ■

S4. ESTIMATING THE QUANTUM FISHER INFORMATION BASED ON THE FIDELITY WITH RESPECT TO DICKE STATES

In this section, we show that if the fidelity with respect to the Dicke state (S18) is larger than a bound then $\mathcal{F}_Q[\varrho, J_y] > 0$. Moreover, we have seen in Fig. 1(b) that the lower bound on $\mathcal{F}_Q[\varrho, J_y]$ as a function of the fidelity F_{Dicke} normalized by N^2 is not the same curve for all N. In this section, we demonstrate by numerical evidence that the lower bound normalized by N^2 collapses to a nontrivial curve for large N.

As a first step, let us consider the state completely polarized in the y-direction

$$|\Psi_y\rangle = |1\rangle_y^{\otimes N}. \tag{S16}$$

The state (S16) does not change under a rotation around the y-axis, hence $F_Q[\varrho, J_y] = 0$. Its fidelity with respect to the Dicke state (10) is

$$F_{\text{Dicke}}(|\Psi_y\rangle) = \frac{1}{2^N}\binom{N}{N/2} \approx \sqrt{\frac{2}{\pi N}}. \tag{S17}$$

From convexity of the bound on the quantum Fisher information in F_{Dicke}, it immediately follows that for F_{Dicke} smaller than Eq. (S17) the optimal lower bound on $F_Q[\varrho, J_y]$ will give zero. For the examples shown in Fig. 1(b), this fidelity limit is 0.3125 and 0.1254 for $N = 6$ and $N = 40$, respectively.

Next, we examine what happens if the fidelity is larger than Eq. (S17).

Observation S2.—If for some state ϱ we have

$$F_{\text{Dicke}}(\varrho) \equiv \text{Tr}(|D_N\rangle\langle D_N|\varrho) > F_{\text{Dicke}}(|\Psi_y\rangle), \tag{S18}$$

then $\mathcal{F}_Q[\varrho, J_y] > 0$. [The state $|D_N\rangle$ is given in Eq. (10), and $F_{\text{Dicke}}(|\Psi_y\rangle)$ is given in Eq. (S17).]

Proof. We have to determine maximum for $F_{\text{Dicke}}(\varrho)$ for states that are not useful for metrology, i.e., $\mathcal{F}_Q[\varrho, J_y] = 0$. We know that $\mathcal{F}_Q[\varrho, J_y]$ is the convex roof of $4(\Delta J_y)^2$ [42]. Hence, if we have a mixed state for which $\mathcal{F}_Q[\varrho, J_y] = 0$, then it can always be decomposed into the mixture of pure states $|\Psi_k\rangle$ for which $\mathcal{F}_Q[\Psi_k, J_y] = 0$. As a consequence, the extremal states of the set of states for which $\mathcal{F}_Q[\varrho, J_y] = 0$ are pure states, and we can restrict our search for pure states. The optimization problem we have to solve can be given as

$$\max_{|\Psi\rangle:\mathcal{F}_Q[|\Psi\rangle,J_y]=0} |\langle\Psi|D_N\rangle|^2. \tag{S19}$$

Pure states $|\Psi\rangle$ for which $\mathcal{F}_Q[|\Psi\rangle, J_y] = 0$ must be invariant under $U_\phi = \exp(-iJ_y\phi)$ for any ϕ. Such states are the eigenstates of J_y. In order to maximize the overlap with the symmetric Dicke state $|D_N\rangle$ in Eq. (S19), we have to look for symmetric eigenstates of J_y. These are the symmetric Dicke states in the y-basis $|\text{D}_N^{(m)}\rangle_y$, where symmetric Dicke states in the z-basis are given in Eq. (9). In order to procceed, we have to write down $|\text{D}_N^{(m)}\rangle_y$ in the z-basis. Then, using the formula

$$\sum_k \binom{n}{k}\binom{n}{q-k}(-1)^k = \begin{cases} \binom{n}{q/2}(-1)^{q/2} & \text{for even } N, \\ 0 & \text{for odd } N, \end{cases} \tag{S20}$$

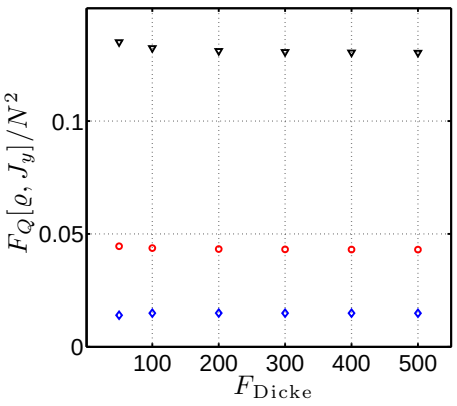

FIG. S1. The lower bound on $F_Q[\varrho, J_y]$, denoted by $\mathcal{B}(F_{\rm Dicke})$, for various particle numbers (diamonds) for $F_{\rm Dicke} = 0.2$, (circles) 0.5, and (triangles) 0.8. For $F_{\rm Dicke} = 0.2$, 10 times the calculated values are shown for a better visibility.

one finds that the squared overlap is given by

$$|\langle \mathrm{D}_N^{(N/2)}|\mathrm{D}_N^{(m)}\rangle_y|^2 = \begin{cases} \frac{\binom{N/2}{m/2}^2\binom{N}{N/2}}{2^N\binom{N}{m}} & \text{for even } N, \\ 0 & \text{for odd } N, \end{cases} \quad \text{(S21)}$$

which is maximal for $m = 0$. ■

Next, we will examine the behavior of our lower bound on $F_Q[\varrho, J_y]$ based on $F_{\rm Dicke}$ for large N. In Fig. S1, the calculations up to $N = 500$ present a strong evidence that for the fidelity values $F_{\rm Dicke} = 0.2, 0.5, 0.8$ the lower bound on the quantum Fisher information $F_Q[\varrho, J_y]$ has a $O(N^2)$ scaling. If this is correct then reaching a fidelity larger than a certain bound for large N would imply Heisenberg scaling for the bound on the quantum Fisher information. Note that it is difficult to present a similar numerical evidence for small values of $F_{\rm Dicke}$, since in that case the bound for the quantum Fisher information is nonzero only for large N due to Observation S2.

S5. BOUNDARY OF PHYSICAL STATES IN THE $(\langle J_z\rangle, \langle J_x^2\rangle)$-PLANE.

In this section, we discuss how to find the physical region in the $(\langle J_z\rangle, \langle J_x^2\rangle)$-plane, which has been used to prepare Fig. 2(a).

The physical region must be a convex one, since the set of quantum states is convex and the coordinates depend linearly on the density matrix. Hence, we look for the minimal/maximal $\langle J_x^2\rangle$ for a given $\langle J_z\rangle$ by looking for the ground states of the Hamiltonians [50]

$$H_{\rm bnd}^{(\pm)}(\mu) = \pm J_x^2 - \mu J_z. \quad \text{(S22)}$$

The points of the boundary can be obtained by evaluating $\langle J_x^2\rangle$ and $\langle J_z\rangle$ for the ground states of Eq. (S22). In particular, the ground states of $H_{\rm bnd}^{(+)}$ correspond to boundary points below the point P corresponding to the fully polarized state in Fig. 2(a). The ground states of $H_{\rm bnd}^{(-)}$ correspond to boundary points above point P.

For $0 < \mu < \infty$, the Hamiltonian $H_{\rm bnd}^{(+)}$ has nondegerate ground states with $\langle J_x\rangle = 0$. For even N, the ground state of $H_{\rm bnd}^{(+)}$ minimizes both $\langle J_x^2\rangle$ and $(\Delta J_x)^2$ for a given $\langle J_z\rangle$. For odd N, this is not the case for small μ [50].

On the other hand, $H_{\rm bnd}^{(-)}(\mu)$ has doubly degenerate ground states. For the ground state subspace, we have $\langle J_x\rangle = 0$. Hence, both for even N and odd N, the ground state of $H_{\rm bnd}^{(-)}$ maximizes both $\langle J_x^2\rangle$ and $(\Delta J_x)^2$ for a given $\langle J_z\rangle$.

S6. QUANTUM FISHER INFORMATION FOR STATES AT THE BOUNDARY OF THE PHYSICAL REGION IN THE $(\langle J_z\rangle, \langle J_x^2\rangle)$-PLANE

We will show that, for even N, ground states of $H_{\rm bnd}^{(+)}(\mu)$ defined in Eq. (S22) are close to saturating Eq. (2). As a consequence, for the boundary of the physical region in the $(\langle J_z\rangle, \langle J_x^2\rangle)$-plane below point P in Fig. 2, the bound (2) is close to the optimal lower bound.

We will carry out numerical calculations. Let us denote by $|\Psi_\mu\rangle$ the ground state of $H_{\rm bnd}^{(+)}(\mu)$. Moreover, let us denote the relevant expectation values for this state by $\langle J_x^2\rangle_\mu$ and $\langle J_z\rangle_\mu$. We know that under the constraint $\langle J_z\rangle = \langle J_z\rangle_\mu$, the state $|\Psi_\mu\rangle$ minimizes $\langle J_x^2\rangle$. For $H_{\rm bnd}^{(+)}(\mu)$, the ground state is unique for $0 < \mu < \infty$. Thus, there is no other quantum state with the same value for $\langle J_z\rangle$ and $\langle J_x^2\rangle$.

There is a very important consequence of the uniqueness of the ground state of $H_{\rm bnd}^{(+)}(\mu)$ for the lower bound on the quantum Fisher information. We discussed that our method based on the Legendre transform gives the optimal lower bound for the quantum Fisher information

$$\mathcal{F}_Q[\varrho, J_y] \geq \mathcal{B}(\langle J_z\rangle_\varrho, \langle J_x^2\rangle_\varrho), \quad \text{(S23)}$$

where $\mathcal{B}$ denotes the optimal bound. Since there is a unique state corresponding to the boundary points, we must have for the states at the boundary

$$\mathcal{B}(\langle J_z\rangle_\mu, \langle J_x^2\rangle_\mu) = \mathcal{F}_Q[\Psi_\mu, J_y]. \quad \text{(S24)}$$

Thus, for the boundary points we do not have to compute the lower bound with the method based on the Legendre transform. We can just calculate the right-hand side of Eq. (S24) instead. Since we have a pure state, the quantum Fisher information is proportional to the variance $\mathcal{F}_Q[\varrho, J_y] = 4(\Delta J_y)^2$ [11].

We add that, as noted in Sec. S4, for even N, the state Ψ_μ not only minimizes $\langle J_x^2\rangle$ for a given value of $\langle J_z\rangle$, but it also minimizes, and this state is unique $(\Delta J_x)^2$ [50].

Hence, for the points on the boundary of physical states in the $(\langle J_z\rangle, (\Delta J_x)^2)$-space we have

$$\mathcal{B}(\langle J_z\rangle_\mu, (\Delta J_x)^2_\mu) = \mathcal{F}_Q[\Psi_\mu, J_y], \tag{S25}$$

where $\mathcal{B}$ denotes the optimal bound if the expectation value $\langle J_z\rangle$ and the variance $(\Delta J_x)^2$ are constrained. Note that the bound (S25) is monotonous in $(\Delta J_x)^2_\mu$ [50].

In Fig. 2(b), we plotted the relative difference between the quantum Fisher information of $|\Psi_\mu\rangle$ and the lower bound (2)

$$\frac{(\Delta\mathcal{F}_Q)_\mu}{\mathcal{F}_Q[\Psi_\mu, J_y]} \equiv \frac{\mathcal{F}_Q[\Psi_\mu, J_y] - \frac{\langle J_z\rangle^2_\mu}{(\Delta J_x)^2_\mu}}{\mathcal{F}_Q[\Psi_\mu, J_y]} \tag{S26}$$

for various particle numbers. It can be seen that for an almost fully polarized state the difference is small, but even for not fully polarized state the relative difference is smaller than 3% for the particle numbers considered.

S7. WHY WE CAN ASSUME $\langle J_x\rangle = 0$ FOR THE DISCUSSION OF SPIN-SQUEEZED STATES

We will show that for the state minimizing $\mathcal{F}_Q[\varrho, J_y]$ for given $\langle J_z\rangle$ and $\langle J_x^2\rangle$ we have $\langle J_x\rangle = 0$. Hence, if we constrain only $\langle J_z\rangle$ and $\left\langle J_x^2\right\rangle$, then we get the same bound as if we constrained $\langle J_z\rangle$ and $\left\langle J_x^2\right\rangle$, and we used an additional constraint $\langle J_x\rangle = 0$.

We have to find a tight lower bound on the quantum Fisher information

$$\mathcal{F}_Q[\varrho, J_y] \geq \mathcal{B}(\vec{w}_\varrho) \tag{S27}$$

where $\vec{w}_\varrho = (\langle J_z\rangle_\varrho, \left\langle J_x^2\right\rangle_\varrho, \langle J_x\rangle_\varrho)$. For any ϱ, we can define a state $\varrho_- = \sigma_z^{\otimes N}\varrho\sigma_z^{\otimes N}$, for which $\vec{w}_{\varrho_-} = (\langle J_z\rangle_\varrho, \left\langle J_x^2\right\rangle_\varrho, -\langle J_x\rangle_\varrho)$. The metrological usefulness of ϱ and ϱ_- are the same, i.e., $\mathcal{F}_Q[\varrho, J_y] = \mathcal{F}_Q[\varrho_-, J_y]$. Then, for any ϱ, we can define a state $\varrho_0 = \frac{1}{2}(\varrho + \varrho_-)$, for which we have $\vec{w}_{\varrho_0} = (\langle J_z\rangle_\varrho, \left\langle J_x^2\right\rangle_\varrho, 0)$. Due to the convexity of the quantum Fisher information, ϱ_0 cannot be better metrologically than ϱ or ϱ_-, that is, $\mathcal{F}_Q[\varrho, J_y] = \mathcal{F}_Q[\varrho_-, J_y] \geq \mathcal{F}_Q[\varrho_0, J_y]$.

Since for any ϱ there is a corresponding ϱ_0 with the above properties, it follows that $\mathcal{B}(\vec{v}_\varrho) = \mathcal{B}(\vec{v}_{\varrho_-}) \geq \mathcal{B}(\vec{w}_{\varrho_0}) = \mathcal{B}(\langle J_z\rangle_\varrho, \langle J_x^2\rangle_\varrho, 0)$. Thus, the worst case bound for given $\langle J_z\rangle$ and $\left\langle J_x^2\right\rangle$ is $\mathcal{B}(\langle J_z\rangle, \left\langle J_x^2\right\rangle, 0)$. Hence,

$$\mathcal{B}(\langle J_z\rangle, \langle J_x^2\rangle) = \mathcal{B}(\langle J_z\rangle, \langle J_x^2\rangle, \langle J_x\rangle = 0), \tag{S28}$$

and our claim is proved.

S8. EXPERIMENTS

Few-particle experiments

In this section, we summarize the experimental results creating Dicke states and GHZ states. The summary of the experiments, the fidelity measured and the corresponding bound on the quantum Fisher information can be seen in Table S1. For the experiments with Dicke states, the lower bound on $\mathcal{F}_Q[\varrho, J_y]/N^2$ is shown, while for the GHZ states we estimate $\mathcal{F}_Q[\varrho, J_z]/N^2$. For the experiment of Ref. [14], the $\mathcal{F}_Q[\varrho, J_y]/N^2$ for the density matrix was $(10.326 \pm 0.093)/N^2 = (0.6454 \pm 0.0058)$. As can be seen in Table S1, this value is larger than what we obtained, however, it was calculated by knowing the entire density matrix, while our bound is obtained from the fidelity alone.

Physical system	Targeted quantum state	Fidelity	$\frac{\mathcal{F}_Q}{N^2} \geq$	Ref.
photons	$\|D_4\rangle$	0.844 ± 0.008	0.358 ± 0.011	[31]
		0.78 ± 0.005	0.281 ± 0.059	[34]
		0.8872 ± 0.0055	0.420 ± 0.009	[14]
		0.873 ± 0.005	0.351 ± 0.006	[60]
	$\|D_6\rangle$	0.654 ± 0.024	0.141 ± 0.019	[32]
		0.56 ± 0.02	0.0761 ± 0.012	[33]
photons	$\|GHZ_4\rangle$	0.840 ± 0.007	0.462 ± 0.019	[25]
	$\|GHZ_5\rangle$	0.68	0.130	[61]
	$\|GHZ_8\rangle$	0.59 ± 0.02	0.032 ± 0.016	[62]
	$\|GHZ_8\rangle$	0.776 ± 0.006	0.3047 ± 0.0134	[27]
	$\|GHZ_{10}\rangle$	0.561 ± 0.019	0.015 ± 0.011	[27]
trapped ions	$\|GHZ_3\rangle$	0.89 ± 0.03	0.608 ± 0.097	[28]
	$\|GHZ_4\rangle$	0.57 ± 0.02	0.020 ± 0.013	[29]
	$\|GHZ_6\rangle$	$\geq 0.509 \pm 0.004$	0.0003 ± 0.0003	[63]
	$\|GHZ_8\rangle$	0.817 ± 0.004	0.402 ± 0.010	[30]
	$\|GHZ_{10}\rangle$	0.626 ± 0.006	0.064 ± 0.006	[30]

TABLE S1. Fidelity values and the corresponding bounds on the quantum Fisher information for several experiments with Dicke states and GHZ states. For experiments targeting Dicke states, bounds on $\mathcal{F}_Q[\varrho, J_y]/N^2$ are shown. The maximal value of this quantity is 0.75 and 0.67 for $N = 4$ and $N = 6$, respectively. For experiments with GHZ states, bounds on $\mathcal{F}_Q[\varrho, J_z]/N^2$ are shown, and, in this case, the maximal value is 1.

The experiments in Refs. [27, 34] are with hyperentangled qubits, while in the rest of the experiments a single qubit is stored in a particle. Ref. [30] describes experiments with $2 - 14$ ions, we presented only the results of two of them. Finally, for the experiment of Ref. [61] we used the fidelity estimated using reasonable assumptions discussed in that paper, while the worst case fidelity is lower.

Many-particle experiments

In this section, we consider cold gas experiments creating spin-squeezed states and Dicke states.

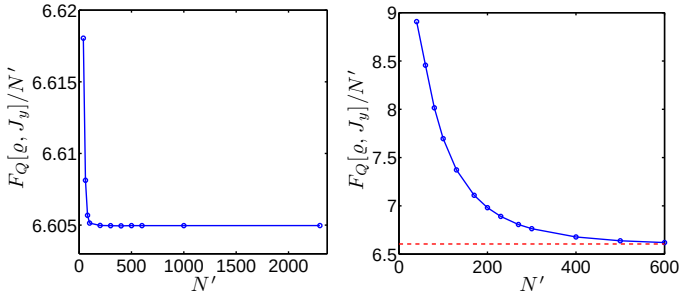

(a) (b)

FIG. S2. Lower bound on the quantum Fisher information based on $\langle J_z\rangle$ and $(\Delta J_x)^2$ obtained for different particle numbers making calculations in the symmetric subspace. $N = 2300$ corresponds to the spin-squeezing experiment of Ref. [7]. (a) Almost fully polarized spin-squeezed state. Even for a moderate N', the bound is practially identical to right-hand side of Eq. (S33). (b) Spin-squeezed state that is not fully polarized. For large N', the bound converges to the right-hand side of Eq. (S33), represented by a dashed line. For details, see text.

Spin-squeezing experiment

We will consider the spin-squeezing experiment of Ref. [7]. The particle number is $N = 2300$, and the spin-squeezing parameter defined as

$$\xi_s^2 = N\frac{(\Delta J_x)^2}{\langle J_z\rangle^2} \tag{S29}$$

has the value $\xi_s^2 = -8.2\text{dB} = 10^{-8.2/10} = 0.1514$. The spin length $\langle J_z\rangle$ has been close to maximal. In our calculations, we choose

$$\langle J_z\rangle = \alpha\frac{N}{2}, \tag{S30}$$

where we take $\alpha = 0.85$. This is somewhat lower that the experimental value, however, helps us to see various characteristics of the method. At the end of the section we will also discuss the results for larger values of α.

Based on Eqs. (S29) and (S30), we have $\langle J_z\rangle = 977.5$ and

$$(\Delta J_x)^2 = \xi_s^2\frac{\langle J_z\rangle^2}{N} = 62.9. \tag{S31}$$

We assume $\langle J_x\rangle = 0$, as the z-direction was the direction of the mean spin in the experiment.

Since the system is very large, we do not make calculations directly for $N = 2300$, but we start with smaller systems. This is motivated as follows. First, we can use the output of an optimization for a smaller particle number as an initial guess for a larger particle number. Second, while we will be able to carry out the calculation for the particle number of the experiment, we will also see that we could even extrapolate the results from calculation from lower particle numbers. This is useful for future application of our method for very large systems.

For our calculations, we transform the collective quantities from N to a smaller particle number N' using the scaling relation

$$\begin{aligned}\langle J_z\rangle &= \frac{N'}{2}\alpha,\\ (\Delta J_x)^2 &= \xi_s^2\frac{N'}{4}\alpha^2.\end{aligned} \tag{S32}$$

We see that for the scaling we consider, for all N' the bound in Eq. (2) is obtained as

$$\frac{\mathcal{F}_Q[\varrho_{N'}, J_y]}{N'} \geq \frac{1}{\xi_s^2} = 6.605. \tag{S33}$$

In order to be able to model large systems, we carried out the calculations for symmetric states. This way we obtain a lower bound on the quantum Fisher information that we will denote by $\mathcal{B}_{\text{sym}}(\langle J_z\rangle_{\varrho_{N'}}, \langle J_x^2\rangle_{\varrho_{N'}})$. As mentioned in the main text, we could obtain a bound for the quantum Fisher information that is valid even for general, not necessarily symmetric states if the matrix in Eq. (5) had non-degenerate eigenvalues. This is not the case for the spin-squeezing problem. However, we still know that the bound obtained with our calculations restricted to the symmetric subspace cannot be smaller than the optimal bound for general states, $\mathcal{B}(\langle J_z\rangle_{\varrho_{N'}}, \langle J_x^2\rangle_{\varrho_{N'}})$. On the other hand, we know that the bound (2) cannot be larger than the optimal bound for general states. These relations can be summarized as

$$\begin{aligned}\mathcal{B}_{\text{sym}}(\langle J_z\rangle_{\varrho_{N'}}, \langle J_x^2\rangle_{\varrho_{N'}}) &\geq \mathcal{B}(\langle J_z\rangle_{\varrho_{N'}}, \langle J_x^2\rangle_{\varrho_{N'}})\\ &\geq \frac{\langle J_z\rangle^2_{\varrho_{N'}}}{(\Delta J_x)^2_{\varrho_{N'}}},\end{aligned} \tag{S34}$$

where on the right-hand side of Eq. (S34) there is just the bound in Eq. (2).

Based on these ideas, we compute the bound $\mathcal{B}_{\text{sym}}(\langle J_z\rangle_{\varrho_{N'}}, \langle J_x^2\rangle_{\varrho_{N'}})$ for the quantum Fisher information for an increasing system size N'. The results can be seen in Fig. S2(a). The bound obtained this way is close to the bound in Eq. (S33) even for small N'. For larger particle number, i.e., $N' > 200$, it is constant and coincides with the bound in Eq. (S33). This also strongly supports the idea that we could have used the results from small particle numbers to extrapolate the bound for N. Since for the experimental particle numbers we obtain that $\mathcal{B}_{\text{sym}}(\langle J_z\rangle_{\varrho_N}, \langle J_x^2\rangle_{\varrho_N})$ equals the bound in (2), we find that for $N' = N$ all the three lower bounds in Eq. (S34) must be equal. Hence, Eq. (2) is optimal for the experimental system considered in this section. Besides, these results present also a strong argument for the correctness of our approach.

We now give more details of the calculation. We were able to carry out the optimization up to $N' = 2300$ with a usual laptop computer using the MATLAB programming

language [52]. We started the calculation for each given particle number with the r_k parameters obtained for the previous simulation with a smaller particle number.

Let us consider a spin-squeezed state that is not fully polarized and $\alpha = 0.5$. In Fig. S2(b), we can see that for small particle numbers we have a larger bound on $\mathcal{F}_{\mathcal{Q}}[\varrho, J_y]$ than the one obtained from Eq. (2), while for large particle numbers we approach Eq. (2). Note that our calculations in this section were made for symmetric systems, while the calculations in the main text have been done for general, not necessarily symmetric states.

After seeing the results of the calculations for $\alpha = 0.85$ and $\alpha = 0.5$, the question arises, what would be the result for larger α, that is for even more polarized states. It turns out that if we choose α larger that 0.85, then the convergence of $\mathcal{F}_Q[\varrho_{N'}, J_y]/N'$ will even be faster than in Fig. S2(a), and for the particle number of the experiment we obtain again that Eq. (2) is saturated.

Finally, we add a note on a technical detail. We carried out our calculations with the the constraints on $(\Delta J_x)^2$, and $\langle J_z \rangle$, with the additional constraint $\langle J_x \rangle = 0$. For the experimental particles numbers, one can show that our results are valid even if we constrained only $(\Delta J_x)^2$ and $\langle J_z \rangle$, and did not use the $\langle J_x \rangle = 0$ constraint. This way, in principle, we could only get a bound that is equal to one we obtained before or lower. However, we obtained before a value identical to the analytical bound (2). The optimal bound cannot be below the analytic bound, since then the analytic bound would overestimate the quantum Fisher information, and it would not be a valid bound. Hence, even an optimization without the $\langle J_x \rangle = 0$ constraint could not obtain a smaller value than our results.

Experiment creating Dicke states

In order to estimate the metrological usefulness of states created in such experiments, we choose to measure $W_1 = J_x^2$, $W_2 = J_y^2$, and $W_3 = J_z^2$ since the expectation values of these operators uniquely define the ideal Dicke state, and they have already been used for entanglement detection [37]. In cold gas experiments of nowadays, the state created is invariant under transformations of the type $U_z(\phi) = \exp(-iJ_z\phi)$ [19]. For such states $\langle J_x^2 \rangle = \langle J_y^2 \rangle$, which we also use as a constraint in our optimization.

In a way analogous to the derivation of Sec. S6, it can be proved that we do not have to add the constraints $\langle J_l \rangle = 0$ for $l = x, y, z$ explicitly, besides constraining $\langle J_l^2 \rangle$. The lower bound will be the same, as if we had six constraints including $\langle J_l \rangle = 0$.

Figure S3 shows the results for $N = 6$ particles for symmetric states for which

$$\langle W_1 + W_2 + W_3 \rangle = \tfrac{N}{2}(\tfrac{N}{2} + 1) =: \mathcal{J}_N. \tag{S35}$$

It can be seen that the lower bound on quantum Fisher information is the largest for $\langle J_z^2 \rangle = 0$. It reaches the value corresponding to the ideal Dicke state, $N(N + 2)/2 = 24$. It is remarkable that the state is also useful for metrology if $\langle J_z^2 \rangle$ is very large. In this case $\langle J_x^2 \rangle$ and $\langle J_y^2 \rangle$ are smaller than $\langle J_z^2 \rangle$, and this cigar shape uncertainty ellipse can be used for metrology.

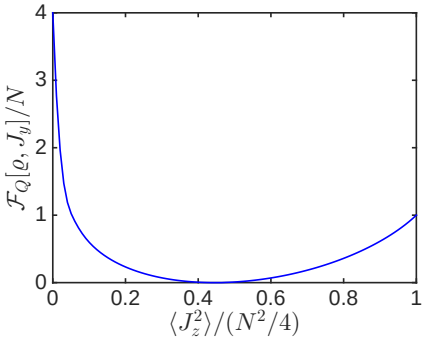

FIG. S3. Optimal lower bound on the quantum Fisher information for symmetric states close to Dicke states for $N = 6$.

After discussing a small system, we will consider an experiment creating Dicke states in Bose-Einstein condensates of cold atoms [37]. In the following, we will get a rough estimate on the quantum Fisher information using scaling ideas. The experimental data are $N = 7900, \langle J_z^2 \rangle_N = 112 \pm 31, \langle J_x^2 \rangle_N = \langle J_y^2 \rangle_N = 6 \times 10^6 \pm 0.6 \times 10^6$ [19].

As in the previous section, we compute the bound for quantum Fisher information for an increasing system size N'. However, now we will not be able to do the calculation for the experimental particle number, and we will use extrapolation from the results obtained for smaller particle numbers.

In the general, non-symmetric case, we can handle only small problems. Thus, we have to transform the collective quantities such that the corresponding quantum state must be symmetric, i.e., it has to fulfil

$$\langle J_x^2 \rangle_{\mathrm{sym},N} + \langle J_y^2 \rangle_{\mathrm{sym},N} + \langle J_z^2 \rangle_{\mathrm{sym},N} = \mathcal{J}_N, \tag{S36}$$

where $\mathcal{J}_N$ is defined in Eq. (S35). A mapping of this type is the following

$$\langle J_l^2 \rangle_{\mathrm{sym},N} = \gamma \langle J_l^2 \rangle_N \tag{S37}$$

for $l = x, y, z$, where

$$\gamma = \frac{\mathcal{J}_N}{\langle J_x^2 + J_y^2 + J_z^2 \rangle_N}. \tag{S38}$$

Note that $\gamma = 1$ if the original state has been symmetric. For our case, $\gamma = 1.301$. This way, we obtain

$$\begin{aligned} \langle J_z^2 \rangle_{\mathrm{sym},N} &= 145.69, \\ \langle J_x^2 \rangle_{\mathrm{sym},N} &= \langle J_y^2 \rangle_{\mathrm{sym},N} = 7.8 \times 10^6. \end{aligned} \tag{S39}$$

We will now consider a scaling that keeps expectation values such that the corresponding quantum state must be symmetric. Hence, we will use the following relation

$$\begin{aligned}\langle J_z^2\rangle_{\mathrm{sym},N'} &= \langle J_z^2\rangle_{\mathrm{sym},N},\\ \langle J_x^2\rangle_{\mathrm{sym},N'} &= \langle J_y^2\rangle_{\mathrm{sym},N'} = \tfrac{1}{2}(\mathcal{J}_{N'} - \langle J_z^2\rangle_{\mathrm{sym},N'}).\end{aligned} \tag{S40}$$

With Eq. (S40), $\langle J_x^2+J_y^2+J_z^2\rangle_{\mathrm{sym},N'} = \mathcal{J}_{N'}$ holds for all N'. In short, $\langle J_z^2\rangle_{\mathrm{sym},N'}$ remains equal to $\langle J_z^2\rangle_{\mathrm{sym},N}$, while $\langle J_x^2\rangle_{\mathrm{sym},N'}$ and $\langle J_y^2\rangle_{\mathrm{sym},N'}$ are chosen such that they are equal with each other and the state is symmetric. For large N, Eq. (S40) implies a scaling of $\langle J_z^2\rangle = \text{const.}$ and $\langle J_x^2\rangle = \langle J_z^2\rangle \sim N(N+2)/8$.

Let us now turn to central quantities of our paper, the lower bounds on the quantum Fisher information. The quantum Fisher information for $\varrho_{N'}$ is bounded from below as

$$\mathcal{F}_Q[\varrho_{N'}, J_y] \geq \mathcal{B}(\langle J_x^2\rangle_{N'}, \langle J_y^2\rangle_{N'}, \langle J_z^2\rangle_{N'}). \tag{S41}$$

An analogous relation for $\varrho_{\mathrm{sym},N'}$ is

$$\mathcal{F}_Q[\varrho_{\mathrm{sym},N'}, J_y] \geq \mathcal{B}_{\mathrm{sym}}(\langle J_x^2\rangle_{\mathrm{sym},N'}, \langle J_y^2\rangle_{\mathrm{sym},N'}, \langle J_z^2\rangle_{\mathrm{sym},N'}). \tag{S42}$$

Based on the scaling properties of $\langle J_l^2\rangle$ discussed above and Ref. [17] we expect

$$\begin{aligned}&\mathcal{B}_{\mathrm{sym}}(\langle J_x^2\rangle_{\mathrm{sym},N}, \langle J_y^2\rangle_{\mathrm{sym},N}, \langle J_z^2\rangle_{\mathrm{sym},N})\\ &\quad\approx \frac{\mathcal{J}_N}{\mathcal{J}_{N'}}\mathcal{B}_{\mathrm{sym}}(\langle J_x^2\rangle_{\mathrm{sym},N'}, \langle J_y^2\rangle_{\mathrm{sym},N'}, \langle J_z^2\rangle_{\mathrm{sym},N'}),\end{aligned} \tag{S43}$$

which we will verify numerically. Note that for large N, we have $\mathcal{J}_N/\mathcal{J}_{N'} \sim N^2/(N')^2$. Here $\mathcal{B}_{\mathrm{sym}}$ denotes the tight lower bound on $\mathcal{F}_Q[\varrho_{\mathrm{sym},N}, J_y]$.

Now we will obtain the results for the original, non-symmetric case. We will need the following observation.

Observation S3.—For the bounds defined in Eq. (S41) and Eq. (S42)

$$\begin{aligned}&\mathcal{B}(\langle J_x^2\rangle_N, \langle J_y^2\rangle_N, \langle J_z^2\rangle_N)\\ &\qquad\leq \frac{1}{\gamma}\mathcal{B}_{\mathrm{sym}}(\langle J_x^2\rangle_{\mathrm{sym},N}, \langle J_y^2\rangle_{\mathrm{sym},N}, \langle J_z^2\rangle_{\mathrm{sym},N})\end{aligned} \tag{S44}$$

holds, where γ is given in Eq. (S38).

Proof. We know that for the singlet state with $\langle J_l^2\rangle_{\varrho_{\mathrm{singlet},N}} = 0$ we have $\mathcal{F}_Q[\varrho_{\mathrm{singlet}}, J_y] = 0$. Let us consider now the mixture

$$\tilde{\varrho}_N = (1-\tfrac{1}{\gamma})\varrho_{\mathrm{singlet},N} + \tfrac{1}{\gamma}\varrho_{\mathrm{sym},N}. \tag{S45}$$

For this state, $\langle J_l^2\rangle_{\tilde{\varrho}_N} = \langle J_l^2\rangle_N$, which we can be seen from Eq. (S37). Hence, $\tilde{\varrho}_N$ gives the value for the second moments that have been measured experimentally. Hence,

$$\begin{aligned}\mathcal{B}(\langle J_x^2\rangle_N, \langle J_y^2\rangle_N, \langle J_z^2\rangle_N) &\leq \mathcal{F}_Q[\tilde{\varrho}_N, J_y]\\ &\leq \tfrac{1}{\gamma}\mathcal{F}_Q[\varrho_{\mathrm{sym},N}, J_y],\end{aligned} \tag{S46}$$

where the first inequality is due to that our bound is not larger than the quantum Fisher information of any state having the given expectation values. The second inequality in Eq. (S46) is due to the convexity of the quantum Fisher information. Since Eq. (S46) is valid for all quantum states, Eq. (S44) follows. ■

Extensive numerics for small systems show that the inequality in Observation S3 is very close to an equality, hence might be used as a basis for making calculations for non-symmetric states.

Based on Eq. (S43) and Eq. (S44), a relation for the lower bound for the original problem can be obtained from the bound on the symmetric problem with N' particles as

$$\begin{aligned}&\mathcal{B}(\langle J_x^2\rangle_N, \langle J_y^2\rangle_N, \langle J_z^2\rangle_N)\\ &\quad\lessapprox \frac{1}{\gamma}\frac{\mathcal{J}_N}{\mathcal{J}_{N'}}\mathcal{B}_{\mathrm{sym}}(\langle J_x^2\rangle_{\mathrm{sym},N'}, \langle J_y^2\rangle_{\mathrm{sym},N'}, \langle J_z^2\rangle_{\mathrm{sym},N'}).\end{aligned} \tag{S47}$$

In Eq. (S47), the "$\lessapprox$" relation would become "$\leq$", if the scaling formula (S43) central to our derivation were exactly true. In Fig. S4, we plotted the right-hand side of Eq. (S47) as the function of N'. With this method, we obtain a

$$\mathcal{B}(\langle J_x^2\rangle_N, \langle J_y^2\rangle_N, \langle J_z^2\rangle_N) \lessapprox 2.94. \tag{S48}$$

In Fig. S4, we can see that $\mathcal{B}(\langle J_x^2\rangle_{N'}, \langle J_y^2\rangle_{N'}, \langle J_z^2\rangle_{N'})$ is constant or slightly increasing for $N' > 400$. This is a strong evidence that Eq. (S43) is valid for large particle numbers. Based on that, we can use the extrapolation $\mathcal{B}(\langle J_x^2\rangle_N, \langle J_y^2\rangle_N, \langle J_z^2\rangle_N) \approx \mathcal{B}(\langle J_x^2\rangle_{N'}, \langle J_y^2\rangle_{N'}, \langle J_z^2\rangle_{N'})$.

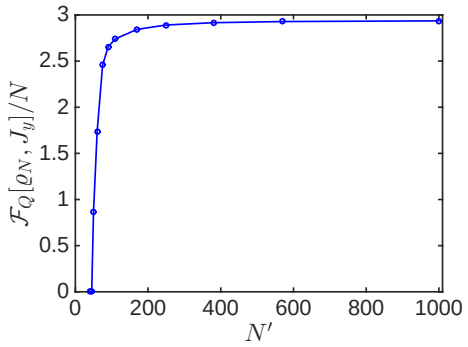

FIG. S4. Quantum Fisher information extrapolated to $N = 7900$ from calculations with different particle numbers N' in an experiment creating Dicke states. For details, see text.

This way, we arrive at the bound for the experimental system

$$\frac{\mathcal{B}(\langle J_x^2\rangle_N, \langle J_y^2\rangle_N, \langle J_z^2\rangle_N)}{N} \lessapprox 2.94. \tag{S49}$$

It is instructive to compare this value to the one obtained in Ref. [19], where the metrological usefulness has been bounded from below based on the second and fourth moments of the collective angular momentum components, and assuming $\langle J_z^2\rangle$ is used for parameter estimation. The result has been $\mathcal{F}_Q[\varrho_N, J_y]/N \geq 3.3$. Our result (S48) is somewhat smaller as we did not use the knowledge of the fourth moment, only the second moments. The closeness of the two results is a strong argument for the correctness of our calculations.

We note on the practical side, that r_1 and r_2 corresponding to the optimum do not change much with N', while r_3 changes linearly. This can be used to obtain the initial r_k for a calculation from the optimal r_k carried our for smaller particle numbers.